Inactivation of the Retinoblastoma Protein by Mutant B-Raf in Malignant Melanoma

Yukiko Kobayashi[1, 2], Takahisa Kobayashi[1, 3], Jiro Kikuchi[1], Ken Futaki[1, 2], Taeko Wada[1], Eiji Kusano[3], Satoru Murata[2], Mamitaro Ohtsuki[2] and Yusuke Furukawa[1]

[1]Division of Stem Cell Regulation, Center for Molecular Medicine; [2]Department of Dermatology; [3]Department of Nephrology, Jichi Medical School, 3311-1 Yakushiji, Shimotsuke, Tochigi 329-0498, Japan

Correspondence should be addressed to: Yusuke Furukawa, M.D., Division of Stem Cell Regulation, Center for Molecular Medicine, Jichi Medical School, 3311-1 Yakushiji, Shimotsuke, Tochigi 329-0498, Japan. Phone: +81-285-58-7400; Fax: +81-285-44-7501; E-mail: furuyu@jichi.ac.jp

Abstract

Although activating mutations of B-Raf are the most common genetic abnormalities in human melanomas[1], the mechanism by which mutant B-Raf transforms melanocytes is poorly understood. Here we show that the retinoblastoma tumor suppressor protein (pRB) is a direct target of B-Raf and is inactivated by phosphorylation in melanomas carrying B-Raf mutations. In contrast, pRB is undetectable in melanomas with wild-type B-Raf. Mutant B-Raf directly interacts with pRB and induces its phosphorylation at serine-249 and threonine-252 (S249/T252). Inhibition of B-Raf activity results in dephosphorylation of pRB at S249/T252 along with other sites in melanoma cells. S249/T252 are phosphorylated earlier than other sites during cell cycle entry of normal melanocytes. Blocking B-Raf activation precluded S249/T252 phosphorylation in mitogen-stimulated melanocytes, which was accompanied by the impaired phosphorylation of pRB at other sites. B-Raf enhanced CDK2-mediated pRB phosphorylation in an *in vitro* kinase assay. These results suggest that B-Raf is an initiating RB kinase, which triggers inactivation of pRB at the earliest step in the cell cycle entry of normal melanocytes, and its activating mutations cause deregulated growth, leading to the development of melanoma.

Text

As malignant melanoma is an extremely aggressive neoplasm with high mortality, considerable effort has been made to understand the molecular basis of the disease[2, 3]. Genetic abnormalities found in melanoma include activating mutations of B-Raf (30-70% of cases), point mutations of N-Ras (10-20%), loss-of-function mutations of p53 and PTEN (10-25%), and mutational activation of CDK4 (less than 5%)[4]. Furthermore, it has been reported that melanoma cells frequently carry loss of chromosomes 9p, 10, and 13, which results in the deletion of Ink4a, PTEN, and pRB, respectively, and gain of chromosomes 11q and 12q, which causes amplification of Cyclin D1 and CDK4, respectively[5, 6].

Recent analyses employing a genome-wide surveillance of DNA copy numbers and mutations have revealed the mutually-exclusive pattern of genetic alterations in melanomas and its relationship to the history of ultraviolet (UV) light exposure[7]. B-Raf mutations are most frequently observed in melanomas arising on the skin with intermittent exposure to UV

light such as those on the trunk, arms, and legs, which rarely show the amplification of Cyclin D1 and CDK4. In contrast, B-Raf has wild-type configuration in the vast majority of melanomas from sun-damaged skin, typically on the face, and those with minimal or no UV exposure (acral and mucosal melanomas). Instead, these melanomas often harbor multiple chromosome abnormalities including loss of chromosome 13, deletion of the Ink4a locus, and CDK4/Cyclin D1 amplification, all of which result in physical or functional inactivation of pRB[8].

The absence of genetic abnormalities directly causing pRB inactivation suggests another mechanism of inactivation in melanomas carrying B-Raf mutation, because the RB-E2F pathway plays a crucial role in melanocyte differentiation[9] and is altered in almost all melanoma cells[10], especially those of acral and mucosal origin[11]. To address this issue, we first investigated the relationship between B-Raf mutation and pRB expression using 10 melanoma cell lines and 11 samples from primary lesions of patients with malignant melanoma. As shown in Fig. 1A, pRB expression was absent or under the detection limit of immunoblotting in 5 out of 10 melanoma cell lines, whereas normal human epidermal melanocytes (NHEM) readily expressed RB protein. In 5 cell lines with intact pRB expression, RB protein was heavily phosphorylated at multiple sites including S249/T252 and serine-780 (Ser780). We concomitantly examined the presence of B-Raf mutations, and found that T1796A substitution of the BRAF gene, which results in a V599E amino acid change, was detected in 6 of the 10 cell lines, whereas there were no mutations in other portions of exon 15, nor anywhere in exon 11 (data not shown). Interestingly, the cell lines harboring B-Raf mutation, except for Malme-3M, expressed intact RB protein, whereas all the cell lines without B-Raf mutation lacked pRB expression (Fig. 1A). The correlation between B-Raf mutation and pRB expression was also observed in primary samples (Fig. 1B shows representative results and the data from all cases are summarized in Table 1). These results indicate that pRB is inactivated in almost all melanoma cells by two mechanisms: hyperphosphorylation in B-Raf mutation-positive cases and loss of protein expression in B-Raf mutation-negative cases.

The coexistence of B-Raf mutation and pRB phosphorylation strongly suggests that activated B-Raf kinase mediates the phosphorylation of pRB in melanoma cells. To substantiate this hypothesis, we treated MM-Ac and MM-RU cells with 5-iodo-3-[(3,5-dibromo-4-hydroxyphenyl) methylene]-2-indolinone (GW5074), a potent cell-permeable B-Raf kinase inhibitor[12, 13], and examined the changes in the phosphorylation status of pRB.

The Raf kinase inhibitor almost completely abrogated pRB phosphorylation at multiple sites including S249/T252 and Ser780 with similar kinetics and extent to the effect on ERK1/2, a bona fide target of B-Raf (Fig. 2A shows the data from MM-RU cells). Cell cycle analysis revealed that G1 arrest was not yet apparent at 24 hours of treatment, when pRB phosphorylation was completely abrogated, indicating that this effect was not a simple consequence of growth arrest (Fig. 2A). As GW5074 targets all members of the Raf family[12, 13], we performed the same experiment using siRNA against B-Raf. Treatment of MM-Ac and G-361 cells with BRAF siRNA reduced the amounts of phosphorylated species of pRB in proportion to the decrease in the abundance of B-Raf protein (Fig. 2B). It is of note that c-Raf, which was not affected by siRNA against B-Raf, is not able to substitute B-Raf for pRB phosphorylation in melanoma cells.

Although these results clearly show that B-Raf is involved in pRB phosphorylation in melanoma cells, it is uncertain whether this effect is direct. To clarify this point, we first examined whether B-Raf physically interacts with pRB in melanoma cells. Co-immunoprecipitation assays revealed that B-Raf and pRB formed a complex in MM-Ac cells, which express mutant B-Raf and intact pRB, whereas the association of the two molecules was not detectable in MM-LH cells, which express normal B-Raf but lack pRB (Fig. 2C). Furthermore, we demonstrated the colocalization of B-Raf and pRB using confocal microscopy (Fig. 2D). Interestingly, the association was observed both in the nuclei and the cytoplasm, implying that B-Raf plays a role in the nuclear export of pRB, another possible mechanism of functional inactivation[14, 15].

To corroborate that mutant B-Raf directly phosphorylates pRB, we carried out two types of *in vitro* kinase assays. First, B-Raf was immunoprecipitated from melanoma cells expressing wild-type B-Raf (MM-LH and RPM-MC) and those expressing mutant B-Raf (MM-Ac and G-361), and subjected to an *in vitro* kinase assay using highly-purified full-length pRB as a substrate. Mutant B-Raf exhibited strong RB kinase activity, which was comparable to that of purified CDK2/Cyclin A complex, whereas the normal counterpart possessed a relatively weak activity (Fig. 3A). Next, we performed the same assay with a combination of recombinant mutant B-Raf kinase (V599E) and purified RB protein, and confirmed the strong activity of mutant B-Raf against pRB, whose specificity was demonstrated by complete inhibition with the Raf inhibitor GW5074 (Fig. 3B, left panel). Taken together, these results support the view that B-Raf acts as RB kinase in melanoma cells.

Next, we sought to identify the site(s) of phosphorylation by B-Raf within the pRB sequence. To this end, we performed nano ESI-MS analysis of B-Raf-phosphorylated pRB as described in Methods. The Mascot search of the obtained MS spectra identified 4 possible phosphorylated tryptic peptides of pRB (Fig. 3C, peaks 1~4). A doubly-charged peak at 819.94 *m/z* (peak 4) corresponded to the peptide 241-254 containing two phosphorylated serine/threonine residues (TAVIPINGpSPRpTPR), whereas the other 3 peaks were considered non-specific because of weak ionic strength. In order to confirm the results of nano ESI-MS analysis, we subjected B-Raf-phosphorylated pRB to immunoblotting with 5 different phosphorylation site-specific antibodies. As shown in Fig. 3B, only the antibody against ppRB-S249/T252 recognized RB protein phosphorylated by B-Raf *in vitro*. No signals were detected by this antibody in untreated pRB and pRB treated with B-Raf in the presence of the Raf inhibitor, indicating the specificity of this experiment. These results strongly suggest that B-Raf preferentially phosphorylates pRB at S249/T252, for which the kinases responsible are unidentified.

Finally, we attempted to clarify the biological significance of B-Raf-mediated phosphorylation of pRB at S249/T252 and its implication in the development of malignant melanoma. For this purpose, we first monitored the order of site-specific phosphorylation of pRB during cell cycle entry of normal human melanocytes. Primary human melanocytes were deprived of growth factors for 24 hours to obtain quiescent cells, and stimulated with growth factors to induce synchronized cell cycle entry. Serial analysis of DNA histograms revealed that quiescent melanocytes started to enter the S phase at 24 hours of stimulation, and became fully cycling at 48 hours (Fig. 4A). During the cell cycle entry of melanocytes, pRB was initially phosphorylated at S249/T252 and S807/S811 (4 h), followed by phosphorylation at Ser780, Ser795, and Ser608 (8 h). This pattern is consistent with previous reports in which CDK3/Cyclin C phosphorylates S807/S811 at G0 exit[16], CDK4/Cyclin D phosphorylates Ser780 and Ser795 at mid G1[17, 18], and CDK2/Cyclin E phosphorylates Ser608 and Ser612 at late G1[19, 20]. To data, however, little is known about the biological significance of and kinases responsible for S249/T252 phosphorylation. Phosphorylation at S249/T252 coincided with the activation of B-Raf, as judged by increased expression and autophosphorylation (Fig. 4B). Blocking B-Raf activation by the Raf inhibitor GW5074 precluded S249/T252 phosphorylation of pRB in mitogen-stimulated melanocytes, which was accompanied by impaired phosphorylation of pRB at other sites including S780 (Fig. 4C). These results indicate that B-Raf-mediated pRB phosphorylation

at S249/T252 occurs very early during the G0/G1 to S phase transition of normal human melanocytes, and may positively affect the later step of pRB phosphorylation catalyzed by CDK/Cyclin complexes. To test the latter notion, we phosphorylated pRB with B-Raf in the presence of cold ATP, and then subjected the pre-phosphorylated pRB to *in vitro* kinase assay with purified CDK2/Cyclin A complex. As shown in Fig. 4D, B-Raf markedly augmented RB kinase activity of CDK2/Cyclin A, suggesting that B-Raf-induced S249/T252 phosphorylation is a prerequisite of further phosphorylation of pRB by CDK/Cyclin complexes. Via this mechanism, mutant B-Raf triggers the inactivation of pRB and subsequent deregulated growth of melanocytes, leading to the development of malignant melanoma. Our findings shed new light on the mechanisms of malignant transformation of human melanocytes by mutant B-Raf, and may provide a clue to the development of a better treatment strategy for malignant melanoma.

Methods

Cell lines and cell culture

The human melanoma cell lines MM-AN, MM-BP, MM-LH, MM-RU, and RPMI-MC were kindly provided by Dr. H. Randolph Byers (Harvard Medical School, Boston, USA)[21], and MM-Ac by Dr. Hiroshi Katayama (Katayama Dermatology Clinic, Gunma, Japan). We purchased HMV-II, Malme-3M, Colo679, and G-361 from ATCC (Manassas, VA, USA), and normal human epidermal melanocytes (NHEM) from Kurabo Biomedicals (Osaka, Japan). NHEM were cultured for 24 hours in Medium154S in the absence of growth factors to induce G0 arrest, and stimulated with growth factors (basic fibroblast growth factor, hydrocortisone, insulin, transferrin, phorbol myristate acetate, heparin, and bovine pituitary extracts) to reenter the cell cycle[22]. Primary samples were obtained from patients admitted to Jichi Medical School Hospital at the time of diagnostic surgery. Human specimens were handled in accordance with the requirements of the institutional review board.

Cell cycle analysis

The cell cycle profile was obtained by staining DNA with propidium iodide in preparation for flow cytometry analysis with the FACScan/CellQuest system (Becton-Dickinson, San Jose, CA). The size of the sub-G1, G0/G1, and S+G2/M fractions was calculated as a percentage

by analyzing DNA histograms using the ModFitLT 2.0 program (Verity Software, Topsham, ME).

Detection of B-Raf mutations

DNA was isolated from melanoma cell lines and primary samples according to the standard methods. Exons 11 and 15 of B-Raf cDNA were amplified by PCR using the following primer pairs: exon 11, sense 5'-TCCCTCTCSGGCATAAGGTAA-3' and antisense 5'-CGAACAGTGAATATTTCCTTTGAT-3'; exon 15, sense 5'-TCATAATGCTTGCTCTGAT AGGA-3' and antisense 5'-GGCCAAAAATTTAATCAGTGGA-3'. PCR products were subjected to direct DNA sequencing after purification.

Immunological procedures

We performed Western blotting, immunoprecipitation-immunoblotting assays, and immunohistochemistry using confocal laser microscopy as previously described[23]. The following antibodies (purchased from Cell Signaling Technology, Beverley, MA unless otherwise stated) were used: anti-pRB (4H1), anti-phosphorylated pRB (Ser249/Thr252) (Santa Cruz Biotechnology, Santa Cruz, CA), anti-phosphorylated pRB (Ser807/Ser811), anti-phosphorylated pRB (Ser780), anti-phosphorylated pRB (Ser795), anti-phosphorylated pRB (Ser 608), anti-phosphorylated pRB (Ser 612) (Calbiochem, San Diego, CA, USA), anti-B-Raf (F-7; Santa Cruz Biotechnology; #07-453; Upstate, Lake Placid, NY, USA), anti-phosphorylated B-Raf (Ser 445), anti-c-Raf, anti-phosphorylated ERK1/2 (Thr202/Tyr204), anti-ERK1/2, and anti-β-actin (C4; ICN Biomedicals, Aurora, OH).

Identification of phosphorylation sites of pRB by nano ESL-MS analysis

Highly-purified full-length RB protein (QED Bioscience, San Diego, CA, USA) was phosphorylated by recombinant mutant B-Raf kinase (V599E) (Upstate) *in vitro* according to the manufacturer's instructions, and resolved on 8% polyacrylamide gels. RB protein was excised from gels after staining with Coomassie Brilliant Blue dye, digested with trypsin, and subjected to nano ESI-MS analysis on a Q-TOF2 mass spectrometer (Micromass MS Technologies, Manchester, UK) equipped with a nanoflow source. Parent ion scanning was performed over the *m/z* range of 250-3500 with collision energy of 5 eV.

Two step *in vitro* kinase assays

Highly-purified full-length RB protein (1 μg) was incubated with 0.1 ng of recombinant mutant B-Raf kinase (V599E) in an appropriate reaction buffer containing cold ATP according to the manufacturer's instructions. After 30 minutes, the reaction was terminated by adding 100 nM 5-iodo-3-[(3, 5-dibromo-4-hydroxyphenyl) methylene]-2-indolinone (GW5074) (Calbiochem). The reaction mixture was diluted in CDK2 reaction buffer, and incubated with 1 U/ml purified recombinant CDK2/Cyclin A complex (New England Biolabs, Beverly, MA, USA) in the presence of [γ^{32}P]ATP for 0, 5, 10, 15, and 20 minutes. Phosphorylated RB proteins were visualized by autoradiography after being resolved on 8% polyacrylamide gels.

Acknowledgments

The authors thank Drs. K. S. Takeuchi, A. Hirao and S. Ookawara (Department of Anatomy, Jichi Medical School) for preparation of microscopic specimens of clinical samples. We are also grateful to Ms. N. Hayashi and I. Nozawa for technical assistance. This work was supported in part by the High-Tech Research Center Project for Private Universities: Matching Fund Subsidy from MEXT 2002-2006, and by grants from the Japan Medical Association, the Mitsubishi Pharma Research foundation, and the Vehicle Racing Commemorative Foundation (to Y. F.).

References

1. Davies, H. et al. Mutations of the BRAF gene in human cancer. Nature 417, 949-954 (2002)
2. Thompson, J. F., Scolyer, R. A. & Kefford, R. F. Cutaneous melanoma. Lancet 365, 687-701 (2005)
3. Soengas, M. S. & Lowe, S. W. Apoptosis and melanoma chemoresistance. Oncogene 22, 3138-51 (2003)
4. Chudnovsky, Y., Khavari, P. A. & Adams, A. E. Melanoma genetics and the development of rational therapeutics. J. Clin. Invest. 115, 813-824 (2005)
5. Bastian, B. C., LeBoit, P. E., Hamm, H., Brocker, E. B. & Pinkel, D. Chromosomal gains and losses in primary cutaneous melanomas detected by comparative genomic hybridization. Cancer Res. 58, 2170-2175 (1998)
6. Bastian, B. C. Understanding the progression of melanocytic neoplasia using genomic analysis: from fields to cancer. Oncogene 22, 3081-3086 (2003)
7. Curtin, J. A. et al. Distinct sets of genetic alterations in melanoma. N Engl. J Med. 353, 2135-2147 (2005)
8. Classon, M. & Harlow, E. The retinoblastoma tumour suppressor in development and cancer. Nat Rev Cancer 2, 910-917 (2002)
9. Carreira, S. et al. Mitf cooperates with Rb1 and activates $p21^{Cip1}$ expression to regulate cell cycle progression. Nature 433, 764-769 (2005)
10. Halaban, R., Cheng, E., Smicun, Y. & Germino, J. Deregulated E2F transcriptional activity in autonomously growing melanoma cells. J. Exp. Med. 191, 1005-1015 (2000)
11. Tanaka, N. et al. Expression of Rb, pRb2/p130, p53, and p16 proteins in malignant melanoma of oral mucosa. Oral Oncol. 37, 308-314 (2001)
12. Lackey, K. et al. The discovery of potent cRaf1 kinase inhibitors. Bioorg. Med. Chem. Lett. 10, 223-226 (2000)
13. Edwards, L. A., et al. Combined inhibition of the phosphatidylinositol 3-kinase/Akt and Ras/mitogen-activated protein kinase pathways results in synergistic effects in glioblastoma cells. Mol. Cancer Ther. 5, 645-654 (2006)
14. Zacksenhaus, E., Bremner, R., Phillips, R. A. & Gallie, B. L. A bipartite nuclear localization signal in the retinoblastoma gene product and its importance for biological

activity. Mol. Cell. Biol. 13, 4588-4599 (1993)

15. Johnson, B. R. et al. A-type lamins regulate retinoblastoma protein function by promoting subnuclear localization and preventing proteasomal degradation. Proc. Natl. Acad. Sci. USA 101, 9677-9682 (2004)
16. Ren, S. & Rollins, B. J. Cyclin C/Cdk3 promotes Rb-dependent G0 exit. Cell 117, 239-251 (2004)
17. Kitagawa, M. et al. The consensus motif for phosphorylation by Cyclin D1-Cdk4 is different from that for phosphorylation by Cyclin A/E-Cdk2. EMBO J. 15, 7060-7069 (1996)
18. Rubin, S. M., Gall, A.-L., Zheng, N. & Pavletich, N. P. Structure of the Rb c-terminal domain bound to E2F1-DP1: A mechanism for phosphorylation-induced E2F release. Cell 123, 1093-1106 (2005)
19. Zarkowska, T. & Mittnacht, S. Differential phosphorylation of the retinoblastoma protein by G_1/S cyclin-dependent kinases. J. Biol. Chem. 272, 12738-12746 (1997)
20. Harbour, J. W., Luo, R. X., Dei Santi, A., Postigo, A. A. & Dean, D. C. Cdk phosphorylation triggers sequential intramolecular interactions that progressively block Rb functions as cells move through G1. Cell 98, 859-869 (1999)
21. Byers, H. R., Etoh, T., Doherty, J. R., Sober, A. J. & Mihm, M. C. Jr. Cell migration and actin organization in cultured human primary, recurrent cutaneous and metastatic melanoma. Am J Pathol 139, 423-435 (1991)
22. Swope, V.B., Medrano, E.E., Smalara, D. & Abdel-Malek, Z.A. Long-term proliferation of human melanocytes is supported by the physiologic mitogens α-melanotropin, endothelin-1, and basic fibroblast growth factor. Exp. Cell Res. 217, 453-459 (1995)
23. Kobayashi, Y. et al. Histone deacetylase inhibitor FK228 suppresses the Ras-MAP kinase signaling pathway by up-regulating Rap1 and induces apoptosis in malignant melanoma. Oncogene 25, 512-524 (2006)

Table 1 Expression of pRB and mutation of BRAF in primary melanoma specimens

pRB expression \ BRAF mutation	+	−
+	2	0
−	1	8

*Using the chi-square test, significant correlation was obtained between BRAF mutation and pRB expression (χ^2=6.525, P<0.05).

Figure Legends

Figure 1 Inactivation of pRB and its relationship to B-Raf mutation in melanoma cells.
(A) Whole cell lysates were prepared from 10 human melanoma cell lines and quiescent primary human epidermal melanocytes (NHEM), and subjected to immunoblot analysis for the expression of pRB and phosphorylated pRB at specific sites. The membrane filters were reprobed with β-actin antibody to verify the equal loading and integrity of samples. The absence or presence of BRAF gene mutation is shown at the top. (B) Expression of pRB was examined by immunohistochemistry using anti-pRB monoclonal antibody (4H1) and chicken antibody to mouse immunoglobulin conjugated with Alexa 488 (Amersham Biosciences) in 11 primary human melanoma samples. We simultaneously isolated DNA from the samples and analyzed mutations of the BRAF gene using PCR-direct sequencing. A point mutation at nt. 1796 (T to A substitution) was detected in 2 out of 2 cases with pRB expression (#0682 and #2687), whereas the BRAF gene was in wild-type configuration in 8 out of 9 cases lacking pRB expression (#4190 and #51919, data not shown for other cases). See Table 1 for summary.

Figure 2 Physical and functional interaction of pRB and B-Raf in melanoma cells.
(A) MM-RU cells were cultured in the presence of 10 μM GW5074 for up to 24 hours. Phosphorylation status of pRB was examined by immunoblotting using phosphorylation site-specific antibodies as indicated (right panel). We monitored the inhibition of cellular B-Raf activity by checking ERK1/2 phosphorylation (p-ERK1/2), and equal loading and integrity of samples by detecting β-actin expression. Cell cycle analysis was performed at 0 and 24 hours of culture (left panel). (B) MM-Ac and G-361 cells were treated with 10 μM siRNA against BRAF and its scrambled control (Santa Cruz Biotechnology) for 24 hours. Phosphorylation status of pRB was examined by immunoblotting using phosphorylation site-specific antibodies as indicated (right panel). We monitored the effect and specificity of siRNA by checking B-Raf and c-Raf expression, respectively. (C) Whole cell lysates from MM-Ac and MM-LH cells were subjected to immunoprecipitation with either preimmune rabbit immunoglobulin (rabbit IgG) or anti-B-Raf polyclonal antibody (Upstate), followed by immunoblotting with anti-pRB (4H1) and B-Raf (F-7) monoclonal antibodies. Coomassie Brilliant Blue staining of the precipitated immunoglobulin heavy chain (IgH) is shown as a

loading control. (D) MM-Ac and MM-LH cells were fixed on glass slides in 4% paraformaldehyde in preparation for confocal microscopy. pRB and B-Raf were double-stained with anti-pRB monoclonal (4H1) and anti-B-Raf polyclonal (Upstate) antibodies, respectively, and appropriate secondary antibodies.

Figure 3 B-Raf phosphorylates pRB at serine-249 and threonine-252 (S249/T252).
(A) B-Raf was immunoprecipitated from melanoma cells without BRAF mutation (MM-LH and RPM-MC) and with BRAF mutation (MM-Ac and G-361), and subjected to *in vitro* kinase assay against purified full-length RB protein (QED Bioscience Inc., San Diego, CA) in the presence of [γ^{32}P]ATP. Phosphorylated pRB was resolved on 8% polyacrylamide gels and detected by autoradiography. Coomassie Brilliant Blue staining of the precipitated immunoglobulin heavy chain (IgH) indicates the same efficiency of B-Raf immunoprecipitation. Recombinant CDK2/Cyclin A complex (New England Biolabs) was used as a positive control. (B) Purified full-length RB protein (250ng/lane) was incubated with 0.05 ng of recombinant mutant B-Raf (V599E) (Upstate) in the absence or presence of 100 nM GW5074 in assay dilution buffer I (Upstate) containing [γ^{32}P]ATP at 30 °C for 30 minutes. Phosphorylated pRB was resolved on 8% polyacrylamide gels and detected by either autoradiography (left panel) or phosphorylation site-specific pRB antibodies (right panel). To verify the equal loading of samples, we performed Coomassie Brilliant Blue staining of the gel (left panel) and immunoblot with anti-pRB antibody (right panel). (C) ESI-MS spectrum in the range of 400-900 *m/z* for tryptically-digested B-Raf-phosphorylated pRB is shown. The Mascot search of the spectra identified 4 possible phosphorylated tryptic peptides (peak 1~4).

Figure 4 B-Raf phosphorylates pRB at the initial step of G0/G1 to S phase transition and facilitates later pRB phosphorylation by CDK/Cyclin complexes in normal human melanocytes.
(A) Cell cycle analysis was performed at the indicated time points in mitogen-stimulated NHEM. (B) Whole cell lysates were prepared at the indicated time points, and subjected to immunoblot analysis for the site-specific phosphorylation and abundance of pRB and the expression and phosphorylation (mobility shift) of B-Raf. (C) Quiescent NHEM were stimulated with growth factors in the absence (-) or presence (+) of 10 μM GW5074, and pRB phosphorylation at S249/T252 and Ser780 was examined at the indicated time points. (D)

We performed a two-step *in vitro* kinase assay as described in Methods to investigate the effects of B-Raf-mediated phosphorylation of pRB on RB kinase activity of CDK2/Cyclin A complex.

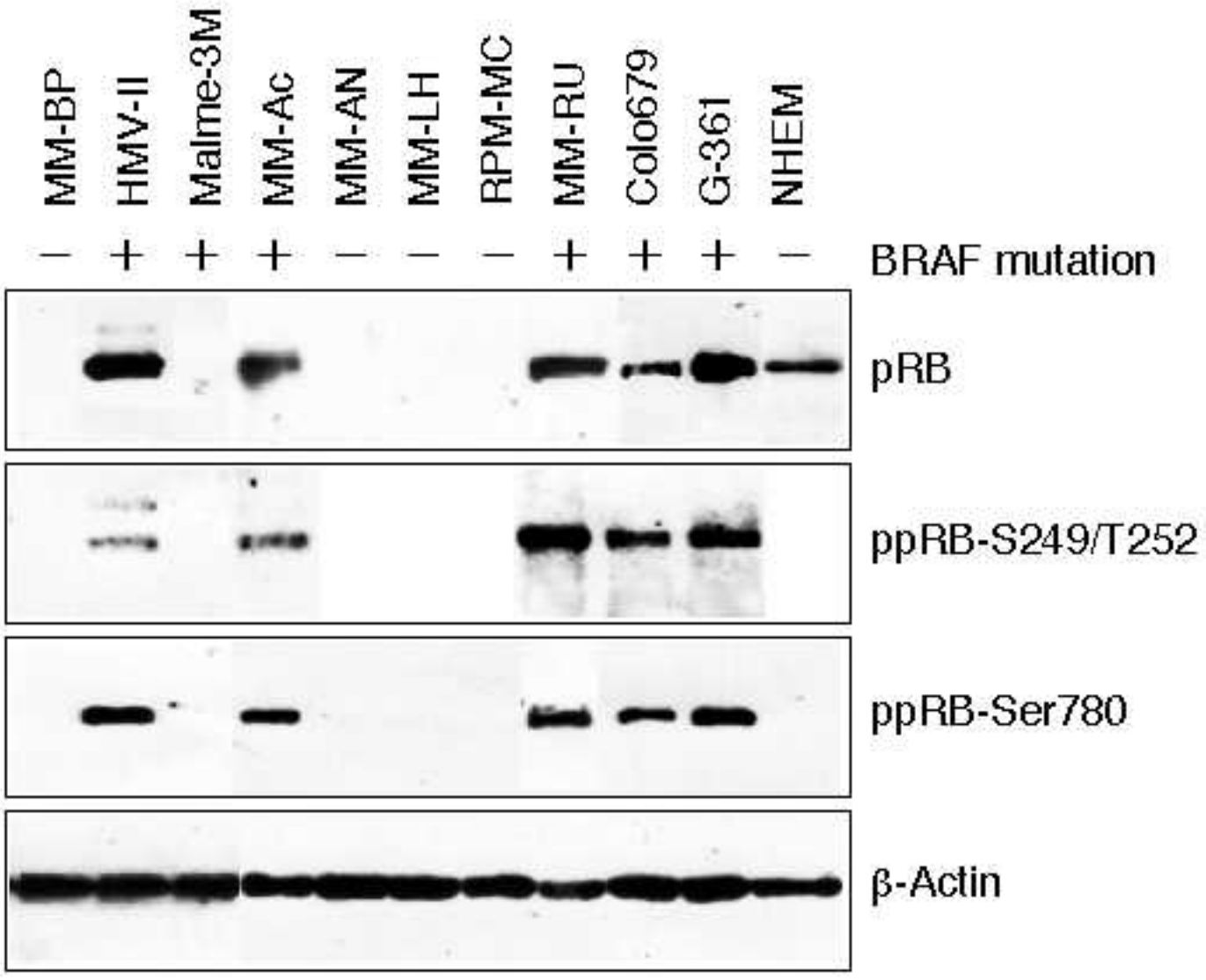

pRB staining

#0682

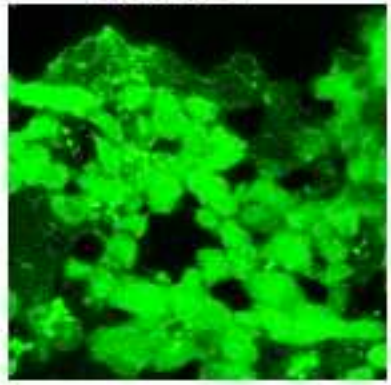

#4190

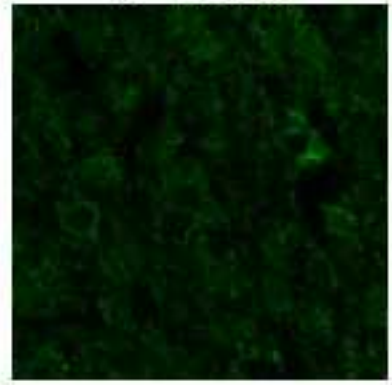

#2687

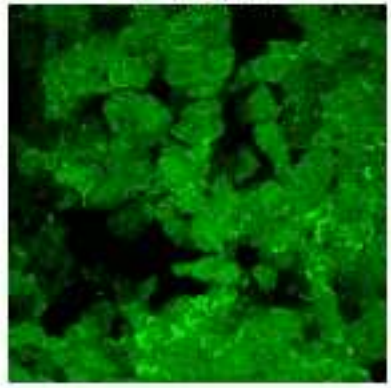

#51919

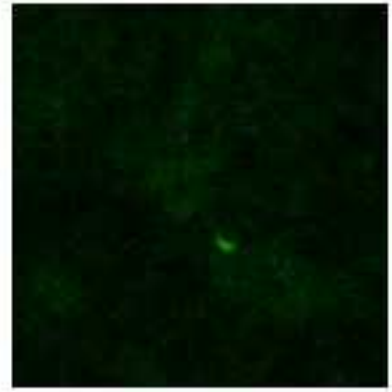

BRAF sequencing

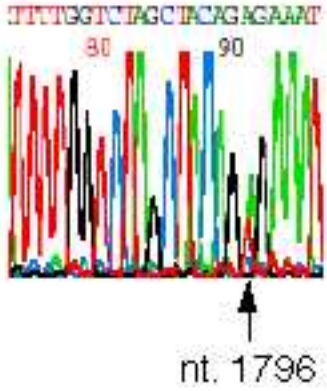

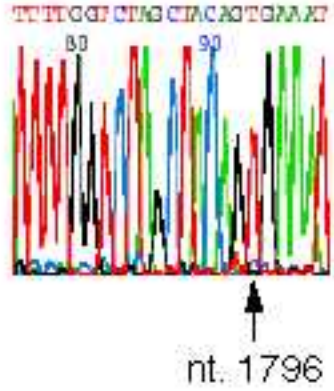

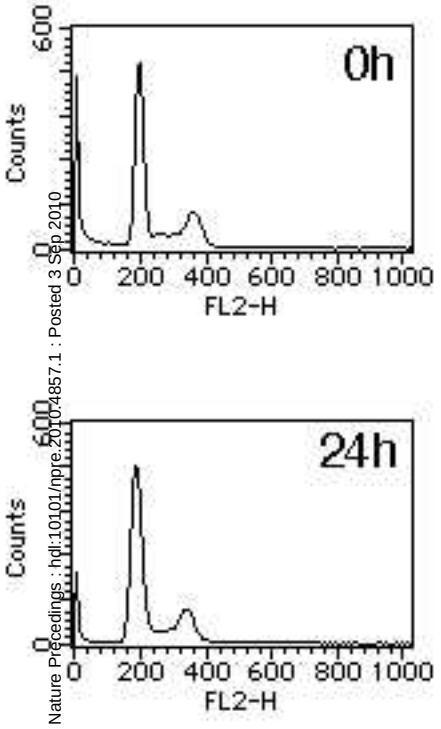

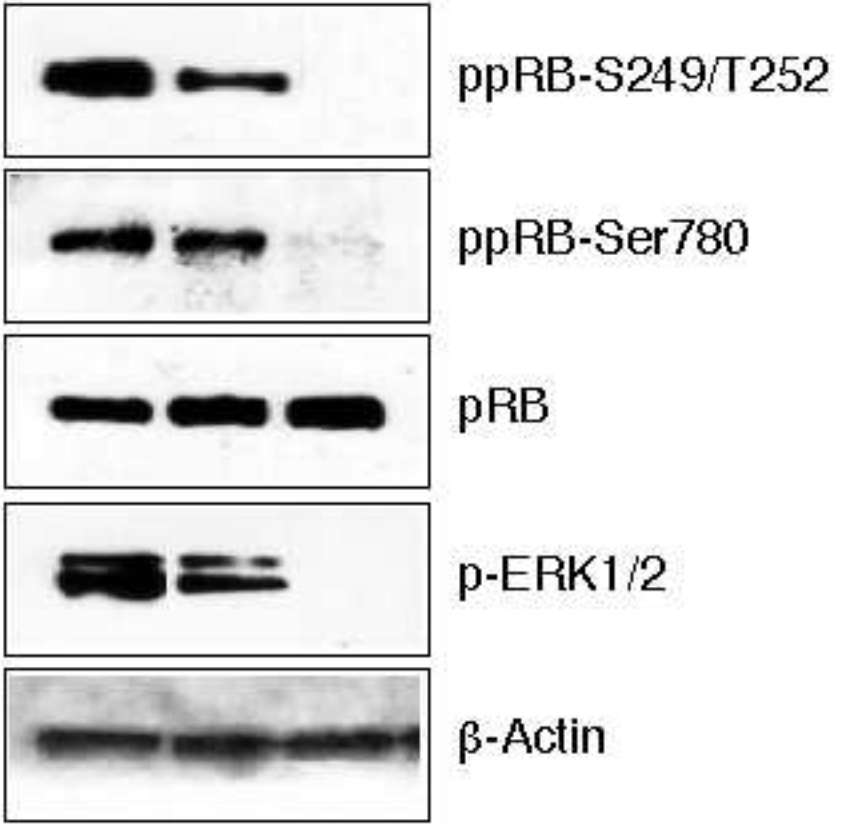

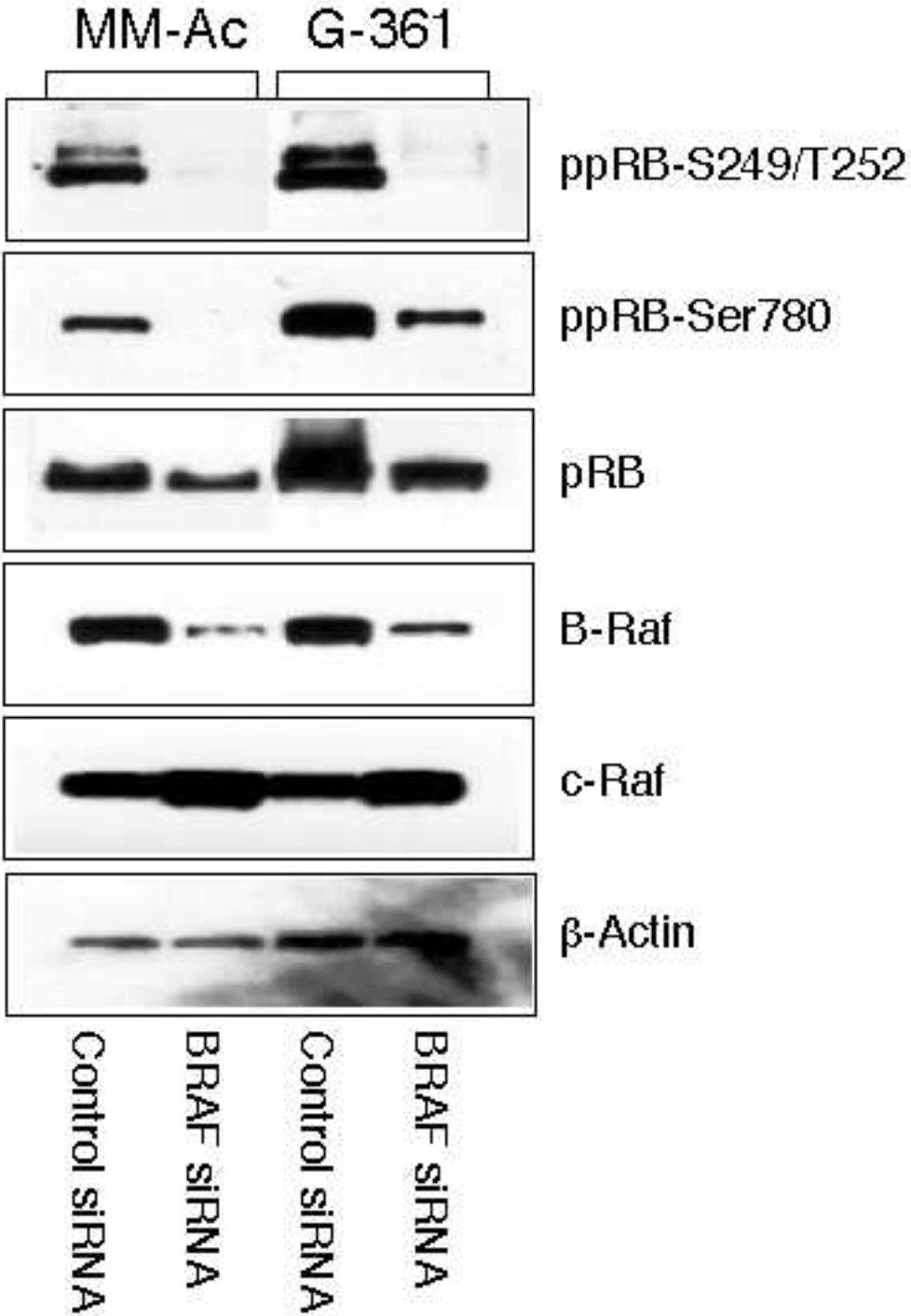

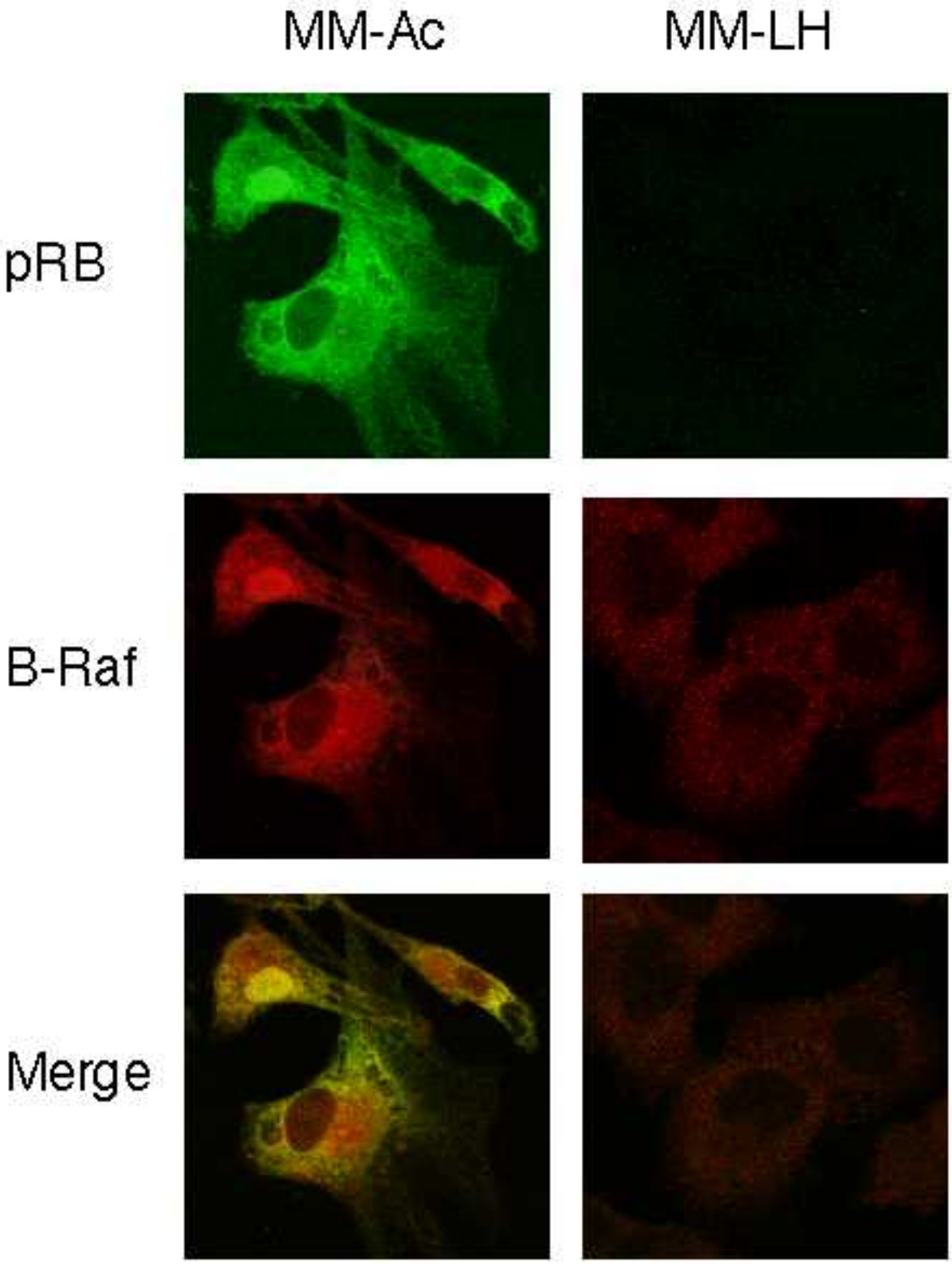

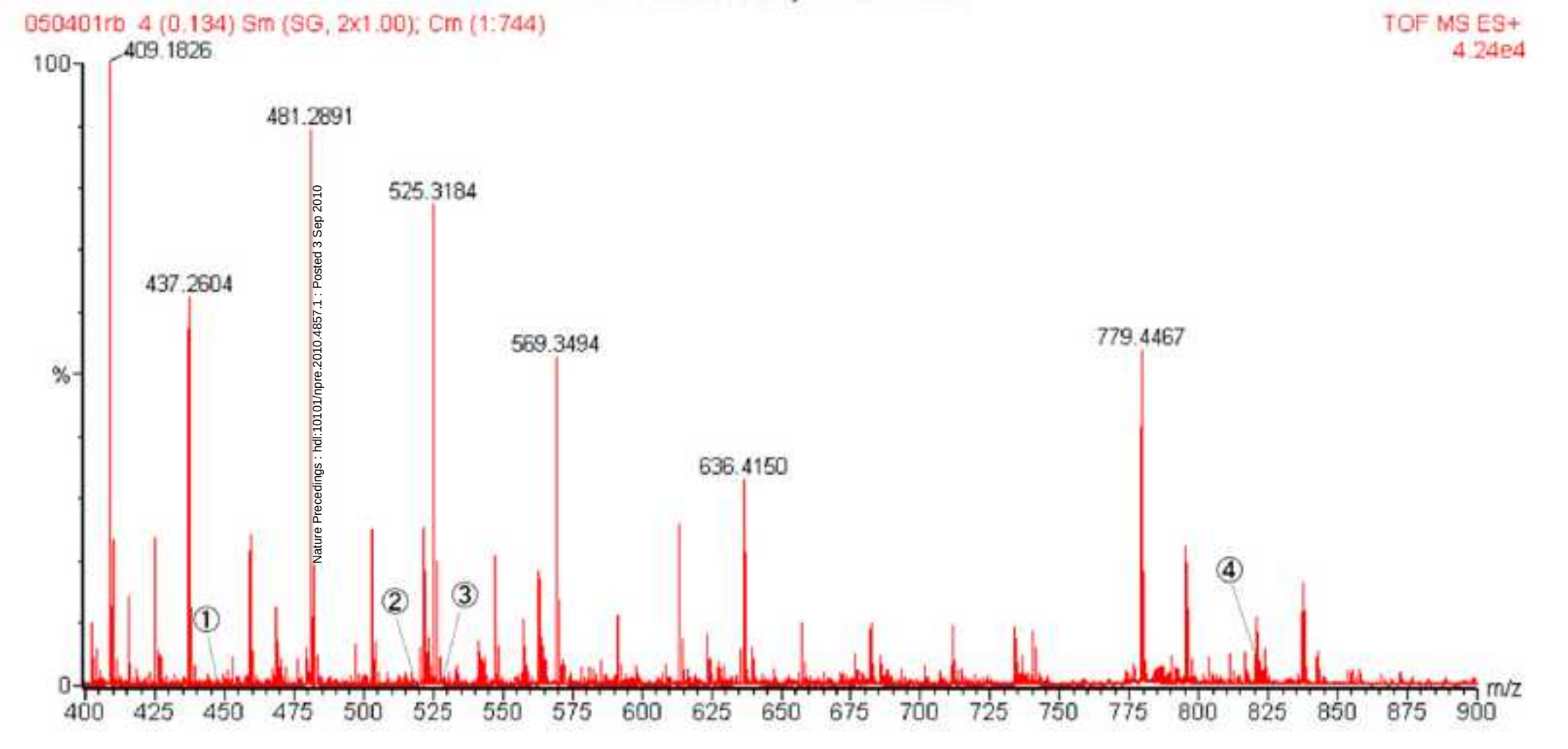

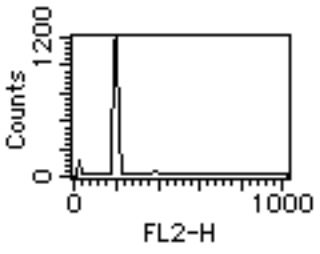

sub-G1: 3.7%
G0/G1: 89.1%
S+G2/M: 8.2%

0

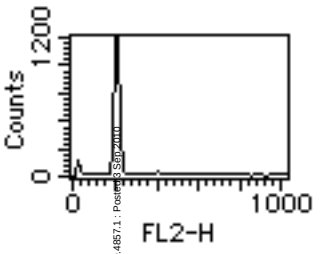

sub-G1: 4.5%
G0/G1: 88.7%
S+G2/M: 6.8%

4

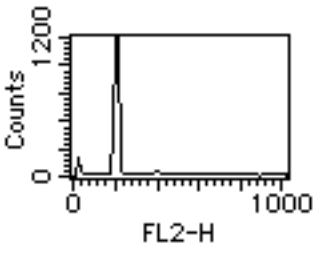

sub-G1: 5.2%
G0/G1: 87.2%
S+G2/M: 7.6%

8

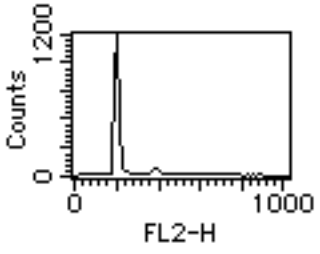

sub-G1: 0.9%
G0/G1: 85.9%
S+G2/M: 13.2%

24

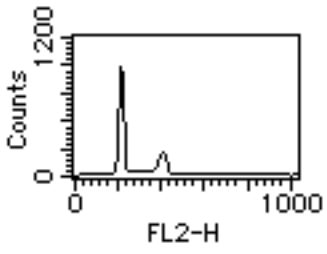

sub-G1: 0.9%
G0/G1: 57.0%
S+G2/M: 42.1%

48

Time in Culture (h)